Simultaneous Separation/Trapping and Dual Trapping of Microparticles in a Novel Microchip using Dielectrophoresis

M.Aghdasi [a], M.Nazari [*, a, b]

[a]Faculty of Mechanical Engineering, Shahrood University of Technology, Shahrood, Iran.
[b]Head of Visualization and Tracking Laboratory (fvt.shahroodut.ac.ir), Shahrood University of Technology, Shahrood, Iran.

PAPER INFO

ABSTRACT

Particle manipulation using Dielectrophoretic (DEP) force is widely used in microfluidic systems. Because this force is highly sensitive to the electrical properties of particles and the medium as well as the frequency of the electric field. Therefore, regarding the electrical properties of particles and the medium, the attractive and repulsive DEP forces can be created by adjusting the electric field frequency. In this numerical study, two electric fields with different frequencies are employed for simultaneous separating/trapping of particles and dual trapping of particles by taking advantage of the DEP force. At first, by proposing a single-chamber microchannel, the effects of frequency and voltage are investigated for trapping the 5μm Polystyrene particles within the microchannel chamber and for separating and ejecting the 2μm polystyrene particles from the microchannel. At this stage, the optimum voltages are obtained for trapping the 5μm particles and ejecting the 2μm particles according to the obtained performance diagrams. Then, another chamber is added to the microchannel for dual trapping of polystyrene particles. By utilizing the optimum voltages, the particles with different sizes are trapped in different chambers of microchannel. In this section, the performance cartography of the proposed system is also evaluated for the first time to select the optimum values and smart separation. In all numerical simulations, two electric fields with different frequencies are used, one electric field absorbs the particles and the other field repels the particles.

1. Introduction

Nowadays, the manipulation of particles is of great importance in different fields of medicine and biotechnology [1-4]. A lot of research has recently been conducted on designing the nano and micro systems for the manipulation of bio-particles by using electrokinetic forces [5-8]. Generally speaking, electrokinetic forces cause the particles to move in the fluid in the presence of electric field [9].

The electric field can generate electrophoresis and dielectrophoretic forces in the particles. The charged particles experience the electrophoresis force in the uniform or non-uniform electric field, while the dielectrophoretic force is generated in the polarizable particles in the non-uniform electric field [10]. Although both of these forces are important, the dielectrophoretic force is employed in this study. A neutral particle polarizes when it is placed in an electric field. Consequently, positive charges accumulate on one side of the particle and negative charges on its other side. The trap of electric charges on both sides of the particle is not equal in a non-uniform electric field. Therefore, in this case, the resultant of forces on the particle is not zero and the particle experiences a pure force. If the particle is more polarizable than its surroundings, this pure force is in the direction of the stronger electric field, and if the surrounding media is more polarizable than the particle, the pure force is towards the weaker electric field. Thus, they are known as positive and negative dielectrophoretic forces, respectively [11,12].

Cui et al. [13] carried out an experimental-analytical study to separate the particles by using a pulse-like electric field. In the area of biomechanics, Ye et al. [14] performed a numerical modeling for the separation of cytoplasm cells with different electrical properties. In this study, lateral electrodes were utilized to separate the particles. Yousuff

[*]Corresponding Author: M. Nazari, Faculty of Mechanical Egineering, Shahrood University of Technology, Shahrood, Iran.
Email: mnazari@shahroodut.ac.ir

et al. [15] conducted a numerical modeling to separate white blood cells from the mixture of blood cells. In this study, the white blood cells were separated by 100% efficiency through adjusting the voltage and flow rate. Piacentini et al. [16] succeeded in separating platelets from red blood cells by using DEP force and a secondary flow. Zhang et al. [17] invented an innovative method for the separation of particles with the aid of external DEP force and an inertial force in a wavy microchannel. Hajari et al. [18] have utilized oblique and non-parallel electrodes to create non-uniform DEP force. In this system, various sizes of particles are initially moving along the first electrode. As the distance between the two electrodes increases, the DEP force is reduced and particles are released from various points according to their size, and the separation process is performed.

Voldman et al. [19] trapped particles in the space between the electrodes with the utilization of four electrodes generating a positive DEP force. Le et al. [20] used different arrangements of electrodes to trap a flexible circular particle inside a chamber. By employing the DEP chocking technique, Zhou et al. [21], were able to stop a flexible particle near the throat of a converging-diverging channel. In the numerical-experimental study of Gonzalez et al. [22], the impression of the number of insulating posts on polystyrene particle trapping has been investigated. In this study, it has been indicated that the required voltage for trapping the particles is decreased by reducing the number of insulating posts. In most studies, a frequency has been used to manipulate the particles. Demierre et al. [23] took advantage of two frequencies of electric field simultaneously to concentrate the particles in an equilibrium position by using DEP force. Urdaneta and Smela [24] also utilized two electric field frequencies simultaneously to trap yeast particles into a chamber, but the effects of different frequencies, voltages and particle sizes were not studied by authors.

In most studies based on DEP force, trapping and separating of particles have been done separately and by using just one frequency. The purpose of this study is to both separate and trap the particles simultaneously and also to trap two batches of particles at two different locations by employing two electric field frequencies (i.e. dual trapping). In other words, trapping (and separating) two types of particles with different sizes in a single microchannel with high efficiency needs more study and it is the main lack of the current literatures. In the first part of this study, the polystyrene particles (with different sizes, 2μm & 5μm) are separated from each other in a single-chamber microchannel by using two electric field frequencies. The 5 micrometer (μm) particles are trapped inside the chamber, and the 2μm polystyrene particles are driven outside of the microchannel. In this case, the best voltages and frequencies are selected for the highest performance of the system. In the next part, another chamber will be added to the microchannel for the ''dual trapping'' of 2μm and 5μm polystyrene particles. Through using the optimum voltages of the first microchannel, the

5μm polystyrene particles are examined in the first chamber, and the trap performance of 2μm particles is evaluated in the second chamber by changing its voltages.

2. Theory of point-particle approach

In this approach, it is assumed that the presence of the particle does not affect the fluid flow and the electric field. That is to say, the fluid flow and the electric field are modeled in the absence of particles. The rotation of particles and the interaction between particles are also ignored. The $\vec{x}_p$ location of each particle can be attained by integrating the particle velocity over time according to the initial location of particle [25],

$$\vec{x}_p(t) = \vec{x}_0 + \int_0^t \vec{u}_p(\tau)d\tau \tag{1}$$

According the above equation, $\vec{x}_p$, $\vec{u}_p$, t are the initial location of particle, particle velocity and time, respectively. By using Newton's second law, the equation of particle's motion in the presence of the DEP force and the drag force is written as follows [25]:

$$m_p \frac{d\vec{u}_p}{dt} = \vec{F}_{DEP} + \vec{F}_d \tag{2}$$

m_p is the mass of particle, $\vec{F}_d$ is the drag force and $\vec{F}_{DEP}$ is the dielectrophoretic force. The drag force on spherical particles submerged in the fluid is expressed by Stokes' law [26]:

$$\vec{F}_d = C_D(\vec{u} - \vec{u}_p) \tag{3}$$

$$D = 6\pi\mu R \tag{4}$$

In the above equations, R is the radius of particle, $\vec{u}$ is the fluid velocity and μ is the fluid viscosity. For an AC field, the time averaged DEP force is as follows [25]:

$$\langle \vec{F}_{DEP} \rangle = 2\pi\varepsilon_0\varepsilon_f R^3 Re\{f_{CM}\}\nabla\vec{E}_{rms}^2 \tag{5}$$

$\vec{E}_{rms}$ is is the root-mean-square of the applied electric field and ε_f is the relative permittivity of fluid and ε_0 is the permittivity in vacuum. Moreover, in equation (5), f_{CM} is the Clausius-Mossoti factor, which is dependent on the electrical properties of the particles, the media and the frequency of electric field. It is defined as follows:

$$f_{CM} = \frac{\tilde{\varepsilon}_p - \tilde{\varepsilon}_f}{\tilde{\varepsilon}_p + 2\tilde{\varepsilon}_f} \tag{6}$$

$$\tilde{\varepsilon} = \varepsilon_0\varepsilon - j\frac{\sigma}{\omega} \tag{7}$$

In equations (6) and (7), $\tilde{\varepsilon}$ is complex permittivity, σ is electrical conductivity and ω is angular frequency. The angular frequency has a connection with the electric field frequency in terms of $\omega = 2\pi f$. The particle is directed to the stronger electric field, when the real part of the

Clausius-Mossoti factor is positive. Contrarily, the particle is directed to the weaker electric field, when the real part of the Clausius-Mossoti factor is negative. When the frequencies of electric fields and their differences are large enough $(f_1, f_2 \gg 1Hz, |f_1 - f_2| \gg 1Hz)$, the interaction effects of electric fields can be neglected. In such conditions, the DEP force produced by each electric field can be combined together [27].

Equation (2) is a first-order linear differential equation that is easily solvable. Assuming that the initial velocity for the particle is zero, the analytical solution of equation (2) is as follows [28]:

$$\vec{u}_p = (\frac{F_{DEP}}{C_D} + \vec{u})(1 - e^{-(\frac{C_D}{m_p})t}) \tag{8}$$

The exponential term of equation (8) contains the characteristic time of $\frac{C_D}{m_p}$ which is much smaller than the system characteristic time scale.

For a particle with the diameter of 5µm and the density of 1060kg/m3, the characteristic time of exponential term is of the order of 10^{-7} s, while the system characteristic time is of the order of 1s.

Therefore, the exponential term of equation (8) can be ignored. In this situation, the particle velocity is the result of fluid velocity and DEP velocity [28].

$$\vec{u}_p = \frac{F_{DEP}}{C_D} + \vec{u} \tag{9}$$

The particle velocity can easily be calculated by using equation (9) instead of equation (2). To calculate the drag force and DEP, the velocity and the electric field should be determined. To compute the velocity field and the electric field, the solution of continuity equations, Navier-Stokes and Laplace are required.

$$\nabla \cdot \vec{u} = 0 \tag{10}$$

$$\rho(\vec{u} \cdot \nabla)\vec{u} = -\nabla p + \mu \nabla^2 \vec{u} \tag{11}$$

$$\nabla^2 V = 0 \tag{12}$$

In the above equations, p, ρ and μ are the pressure, density and fluid viscosity, respectivly, and V is the electric potential. Through solving the Laplace equation, the electric field can be calculated by the following equation:

$$\vec{E} = -\nabla V \tag{13}$$

The boundary conditions for solving the equations of (10), (11), (12) are represented as follows:

$$\vec{u} = \vec{u}_{inlet} \qquad at\ the\ inlet\ boundary \tag{14}$$

$$p = p_{outlet} \qquad at\ the\ outlet\ boundary \tag{15}$$

$$\vec{u} = 0 \qquad at\ the\ walls \tag{16}$$

$$V = V_{electrode} \quad on\ the\ electrode\ surface \tag{17}$$

$$\vec{n} \cdot (\nabla V) = 0 \qquad at\ the\ insulating\ boundesies \tag{18}$$

It is worth noting that $\vec{n}$ is the normal vector of the surface.

3. Materials and Methods

In this study, the finite element method is used to solve the governing equations. At first, the electric field and the fluid velocity are calculated steadily. After achieving the velocity field and the electric field, the DEP force is obtained by using equation (5). Afterwards, the velocity and the motion path of particles are obtained by taking advantage of equations (9) and (1). Figure 1 illustrates the numerical solution flowchart. To investigate the independence of computational grid and timestep, the magnitude of total force exerted on a 2µm polystyrene particle for three grids and four timesteps along the microchannel length are plotted. Since the electric field gradient near the electrodes and the velocity gradient near the walls are intense, the grid aggregation is higher in these areas. According to Figures 2.a and 2.b, the grid with the number of 45624 and the timestep of 0.05 are used for other modellings. The particles employed in this study are polystyrene particles with the diameters of 2µm and 5µm. The electrical conductivity and the relative permittivity of particles are 2e-4S/m and 2.6, respectively [29]. The electrical conductivity and the relative permittivity of deionized water are 1.5e-4S/m and 78, respectively [29]. Furthermore, the fluid density and viscosity are 1000kg/m3 and 1e-3Pa.s, respectively.
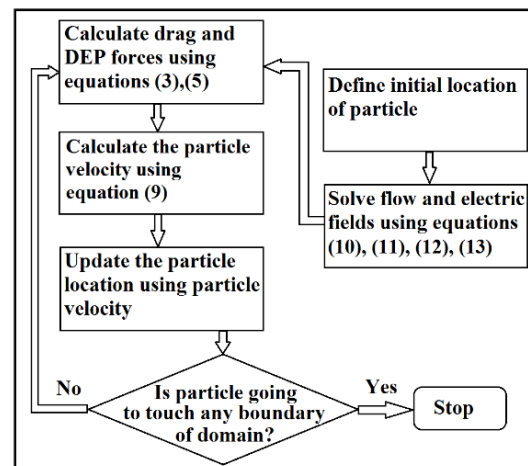

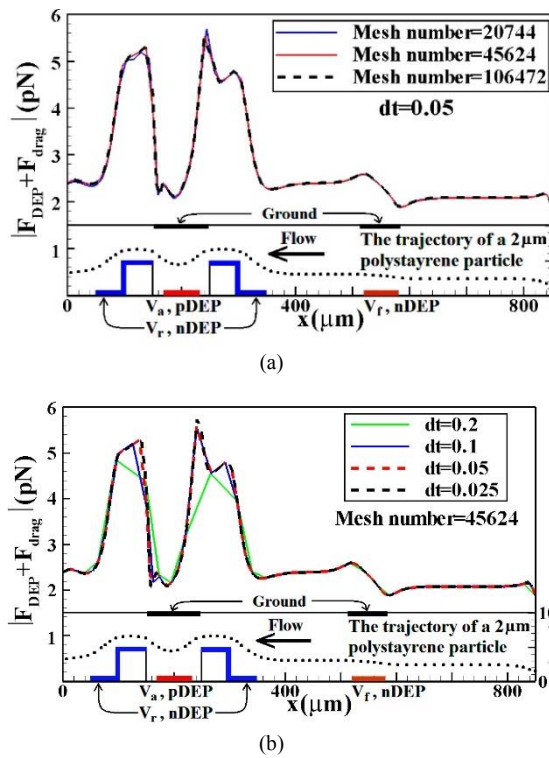**Figure 1.** Numerical Solution Flowchart of the present study

(a)

(b)

Figure 2. The results of independence from (a) the computational grid and (b) timestep $V_p = 8V_{rms}, V_r = 6V_{rms}, V_f = 8V_{rms}, f_{CM} = -0.1$

4. Results and Discussion

4.1. Validation study with numerical and experimental data

In this section, the numerical results of the present study are compared and validated with two studies of Marx et al. [30], and Urdaneta and Smela [24]. Markx et al. [30] conducted an experimental study to levitate polystyrene particles by using DEP force. In this research, the effects of particle diameter, applied voltage, electrode size and electric field frequency on the levitation height were investigated. The numerical results of the present study are compared and validated with the results of Markx et al [30]. Figure 3.a displays the computational domain of numerical modeling and Figure 3.b shows the levitation height of polystyrene particles with 6µm diameter and the electrodes with the width and distance of 20µm. In this case, the maximum error is about 7%. Furthermore, the numerical modeling results of this study are compared and validated with the results of Urdaneta and Smela's study [24]. In an experimental-numerical study, Urdaneta and Smela [24] took advantage of two electric field frequencies simultaneously to trap yeast particles into a chamber. In this research, the negative DEP force was employed to concentrate and push the particles away from the edges of the chamber and the positive DEP force was used to trap the particles into the chamber. Figure 3.d represents the motion path of particles within the microchannel.

Only horizontal lines should be used within a table, to distinguish the column headings from the body of the table, and immediately above and below the table. Tables must be embedded into the text.

4.2. Particle Separation along with Trapping

In this section, two frequencies of electric field have been used simultaneously to trap 5µm polystyrene particles inside the microchannel chamber and to direct 2µm particles outside of the microchannel.

The single-chamber microchannel used in this study is the same as the microchannel that Urdaneta and Smela [24] considered. Figure 4 illustrates the dimensions and location of the electrodes. It should be noted that V_f is the Focusing electrode voltage, V_r is the Repulsive electrode voltage and V_a is the Attractive electrode voltage. The parameters should be studied in order to select the most optimum conditions of trapping the 5µm particles inside the microchannel chamber and ejecting the 2µm particles. To this end, the Focusing voltage varies between $6V_{rms}$ and $11V_{rms}$, the Repulsive voltage changes between $3V_{rms}$ and $6V_{rms}$ and the Attractive voltage alters between $6V_{rms}$ and $12V_{rms}$. Moreover, the frequencies of Focusing and Repulsive electrodes are taken into account 51kHz one time and 70kHz the other time. In these conditions, the Clausius-Mossoti factor is equal to -0.1 and -0.2, respectively. However, the frequency of Attractive electrode is chosen in such a way that the Clausius-Mossoti factor has the highest positive value. The maximum positive value of Clausius-Mossoti factor is 0.166 whose frequency is 1kHz. To examine the performance of the system in various conditions, the performance of trapping the 5µm particles inside the chamber ($\eta_{trapping}$) and the performance of directing the 2µm particles toward the outlet ($\eta_{separating}$) are defined as follows. The 2µm and 5µm polystyrene particles are released freely at the entire input section.

$$\eta_{trapping} = \frac{the\ number\ of\ 5\mu m\ polystyrene\ particles\ trapped\ into\ the\ chamber}{total\ number\ of\ 5\mu m\ polystyrene\ particles\ which\ are\ released} \quad (19)$$

$$\eta_{separating} = \frac{the\ number\ of\ 2\mu m\ polystyrene\ particles\ that\ reached\ the\ exit}{total\ number\ of\ 2\mu m\ polystyrene\ particles\ which\ are\ released} \quad (20)$$

Figures 5.a-f show the results of system ''performance cartography'' for trapping the 5µm particles and ejecting the 2µm particles. In these pictures, the green area indicates the conditions in which all 5µm particles are trapped and all 2µm particles are ejected from the microchannel. For better understanding of the performance diagrams, three points of A, B and C are considered on Figure 5.c that each of these points creates a different performance for the system. Point A, which is located in the green area, displays the circumstances in which all the 5µm polystyrene particles are trapped inside the chamber and all the 2µm polystyrene particles are separated and ejected from the microchannel. The

conditions of B point give rise to the separation and exit of all 2μm polystyrene particles, but about 50% of the 5μm polystyrene particles are trapped. At point C, unlike point B, all 5μm polystyrene particles are trapped inside the chamber, but about 80% of the 2μm particles are separated and ejected from the microchannel. Figure 6 depicts the motion path of particles at point A.

By the enhancement of V_p, the system performance increases for trapping the 5μm particles. In this condition, the exit of 2μm particles decreases. It is because a number of 2μm particles are also trapped into the chamber along with the 5μm particles when V_p increases. The Focusing electrodes reduce the dispersion of particles and concentrate them near the centerline of microchannel by creating the negative DEP force. The Repulsive electrodes also distance the particles from the chamber walls so that

they do not adhere to the walls. Eventually, the Attractive electrodes trap the particles into the chamber.

When V_f is low, the particles do not concentrate well near the centerline of microchannel and the particles, which are away from the chamber, are hardly trapped. Moreover, the particles near the chamber may also adhere to the walls. The system performance increases for trapping the 5μm particles and ejecting the 2μm particle with the augmentation of V_f. It should be noted, however, that the excessive increase of V_f causes the 5μm particles to stop in the area of Focusing electrodes. The increase of V_r causes the particles to recede from the walls and helps the overall performance of the system. The negative DEP force has more intensity when $f_{CM}=-0.2$. Therefore, the Focusing and Repulsive forces increase and the overall performance of the system improves.
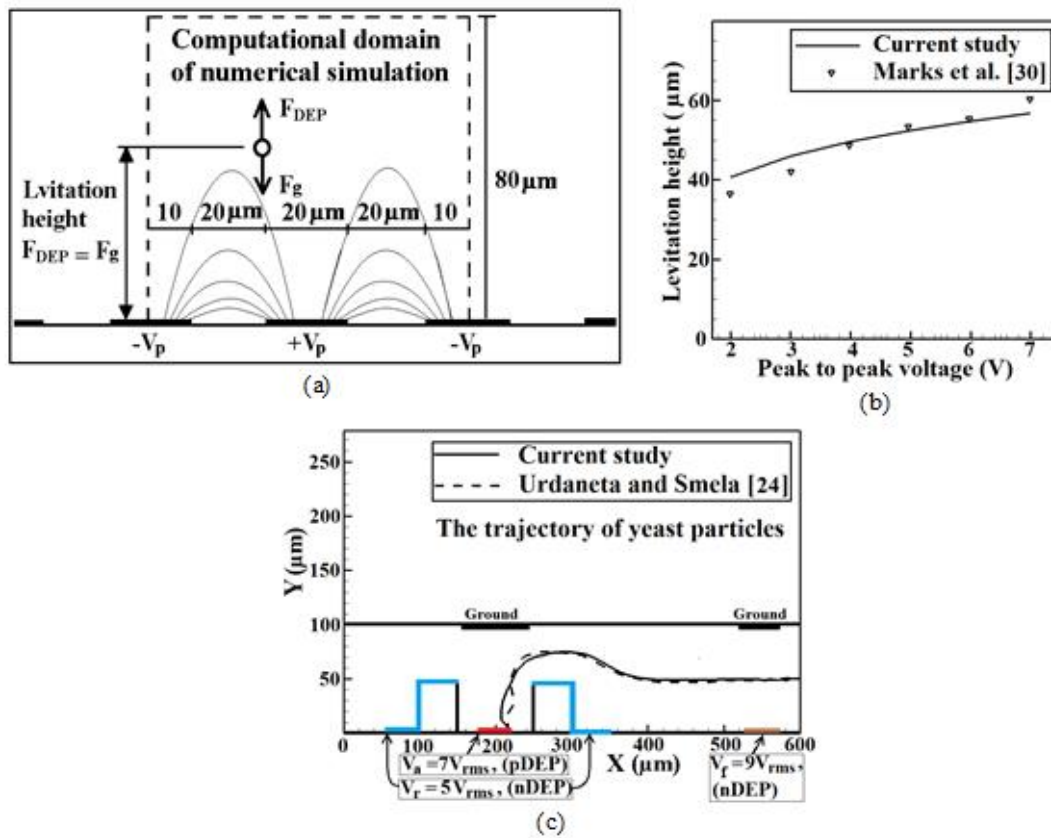

Figure 3. (a) The computational domain of numerical modeling for comparison with the study of Markx et al. [30], the comparison of (b) Levitation height and (c) the motion path of particles with numerical results
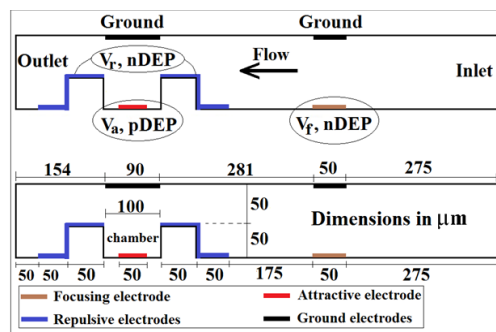

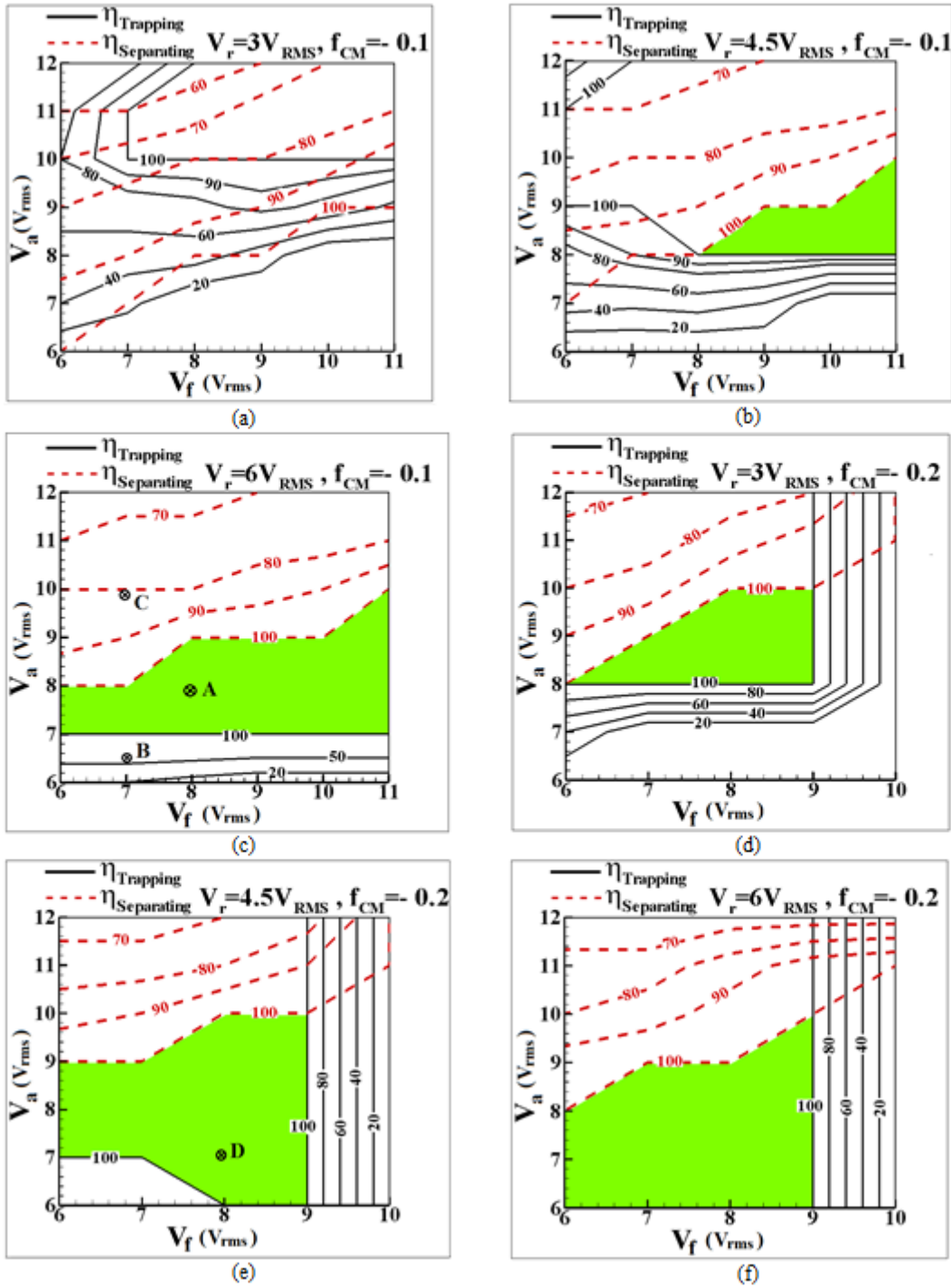**Figure 4.** Microchannel dimensions and the location of electrodes (the sizes are in terms of micrometers)

Figure 5. The functional diagrams (performance cartography) of trapping the 5μm particles (solid lines) and ejecting the 2μm particle (dashed lines)

4.3. Force analysis

In this section, a 5μm polystyrene particle and a 2μm particle are released near the floor of single-chamber microchannel (at 15μm height from the microchannel floor) to facilitate the force analysis. In this situation, the input fluid velocity is 100μm/s, $V_f=7V_{rms}$, $V_p=9V_{rms}$, $V_r=6V_{rms}$ and f_{CM}=-0.1. In these conditions, the 5μm particle is trapped inside the chamber and the 2μm particle is directed to the outside of the microchannel. Multiplying both sides of equation (9) in C_D reveals that the forces that

cause the particle to move are the DEP force and the drag force resulting from the fluid velocity.

$$C_D \vec{u}_p = F_{DEP} + C_D \vec{u} \qquad (21)$$

Figure 7.a shows the normal component of drag forces resulting from the fluid velocity and DEP on the 5μm particle. When the 5μm particle reaches the Focusing electrode, the negative DEP force pushes the particle toward the center of microchannel, which is the weaker

electric field. The drag force is approximately zero in the y direction until the particle reaches near the chamber walls. When the particle reaches near the chamber wall, the drag force and the negative DEP resulting from the Repulsive electrodes act in the same direction and push the particle away from the chamber wall. After the particle passes through the chamber wall, the positive DEP force, which is much stronger than the drag force, traps the particle into the chamber. The 2μm particle, like the 5μm particle, experiences only the negative DEP force resulting from the Focusing electrode until it reaches the chamber wall. In the chamber wall section, the negative DEP force and the drag force push the particle away from the chamber wall. After the particle passes through the chamber wall, the drag force and the positive DEP force, which are obtained from the Attractive electrode, guide the particle into the chamber. However, this force is not sufficient to trap the particle, thus the drag force, whose direction has changed, raises the particles and ejects it from the chamber. Afterwards, the drag force and the negative DEP force distance the particle from the second wall of the chamber and eventually the particle is driven outside of the microchannel (Fig7.b).

The DEP force has a direct relation with the radius cube of particles and the drag force has a direct relation with the radius of particles. Hence, the effect of DEP force is greater than the drag force when the particle's size is larger. For this reason, the 5μm particle, which is inside the chamber, experiences a greater positive DEP force than the 2μm particle and thus it is trapped into the chamber. Figure 8 shows the motion path of particles together with the vectors of drag and DEP forces near the chamber. The gray line indicates the motion path of 5μm particles and the black line depicts the motion path of 2μm particles. The vectors of drag force on the 2μm particle are larger than the vectors of DEP force and the particle keeps moving almost on a streamline. However, the vectors of DEP force on the 5 μm particle are much larger than the vectors of drag force; therefore, the particle does not move on a streamline and is trapped into the chamber. Furthermore, the negative DEP forces at the edges of the chamber walls push the particles away from these areas.

4.4. The dual trapping of polystyrene particles with different sizes

In this section, another chamber is added to the first microchannel to trap the particles at two different points. In this microchannel, the 5μm particles are trapped inside the first chamber and the 2μm particles are trapped inside the second chamber. Figure 9 illustrates the new microchannel and the related electrodes' arrangement. The dimensions of the second chamber are the same as those of the first chamber. The optimum voltages ($V_{p,opt}$, $V_{f,opt}$, $V_{r,opt}$) are selected from the green area of diagrams 5.a-f and only V_{p2} and V_{r2} would be changed. In this situation, the 5μm particles are trapped inside the first chamber with regard to the optimum voltages and it has been attempted to trap the2μm particles inside the second chamber through changing the voltages of V_{p2} and V_{r2}.

It should be noted that the range of changes of V_{p2} and V_{r2} voltages are from $10V_{rms}$ to $14V_{rms}$ and from $10V_{rms}$ to $13V_{rms}$, respectively, and the fluid velocity is 100μm/s as before. According to point D in the diagram of Fig. 5.e, the optimum voltages of Focusing, Repulsive and Attractive electrodes are $8V_{rms}$, $4.5V_{rms}$ and $7V_{rms}$, respectively. Moreover, the Clausius-Mossoti factor is chosen for the electric field with the negative and positive DEP of -0.2 and 0.166, respectively. Figure 10 demonstrates the trap performance of 2μm particles inside the second chamber, whereas all 5μm particles have been trapped inside the first chamber.

The enhancement of V_{p2} and V_{r2} voltages leads to the increase of trapping 2μm particles inside the second chamber. When the 2μm particles reach the second chamber, the force of Attractive electrode at the bottom of chamber on the one hand, and the force of Repulsive electrode on the wall on the other cause the particles to trap into the second chamber. Figure 11 shows the motion path of particles within the microchannel when V_{p2}=$12V_{rms}$ and V_{r2}=$12V_{rms}$. In this situation, the 5μm and 2μm particles have trapped inside the chambers with 100% function.
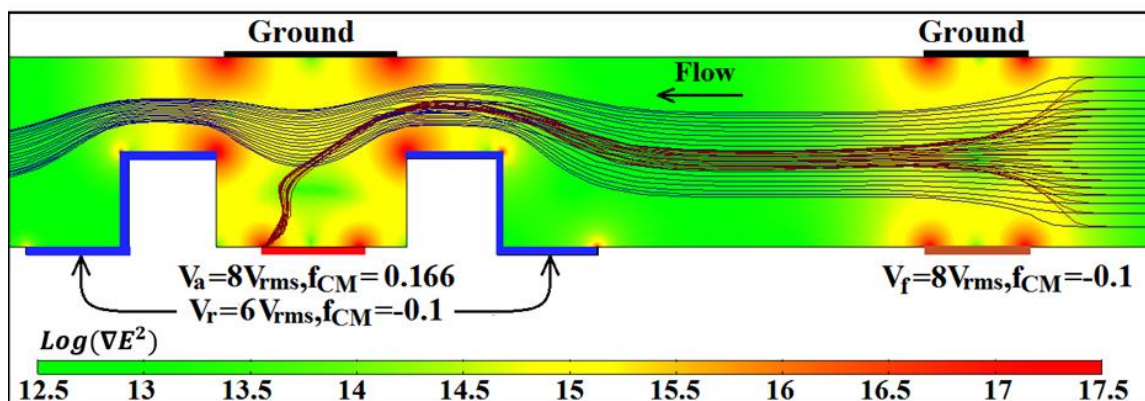

Figure 6. The motion path of 5μm (red) and 2μm (blue) polystyrene particles in the single-chamber microchannel, related to point A of Fig. 5c
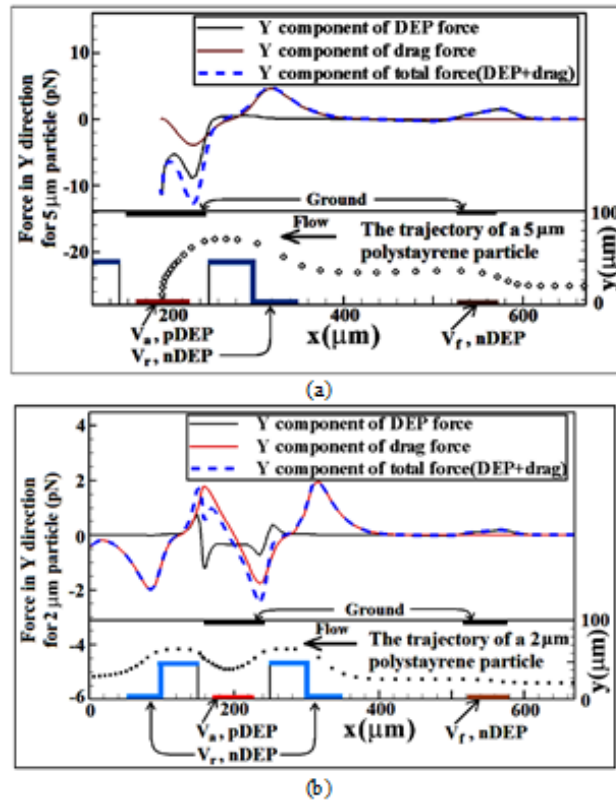
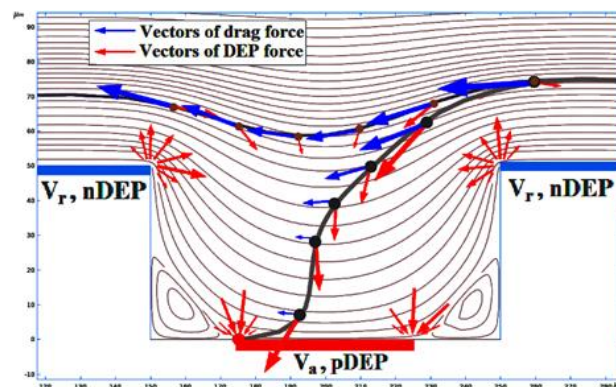**Figure 7.** The normal component of drag force and DEP force applied to (a) 5μm particle (b) 2μm particle

Figure 8. The motion path of 5μm (gray line) and 2um (black line) polystyrene particles with force vectors near the chamber
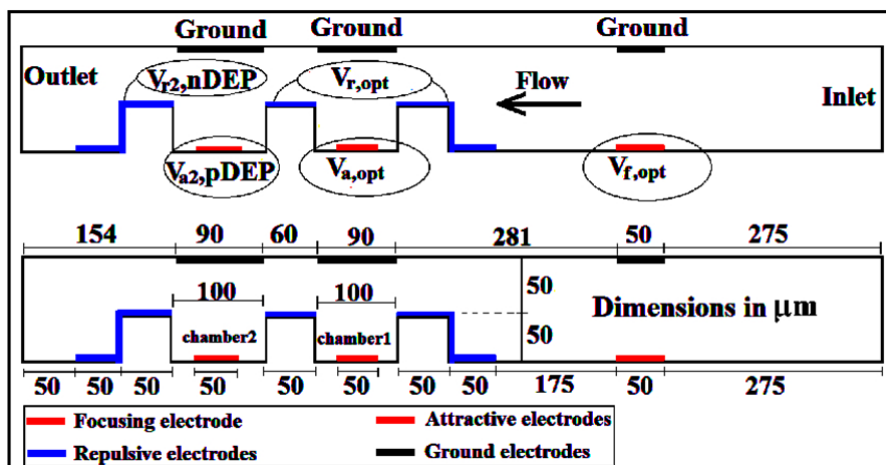

Figure 9. The proposed microchannel and the arrangement of electrodes (sizes are in terms of micrometers)
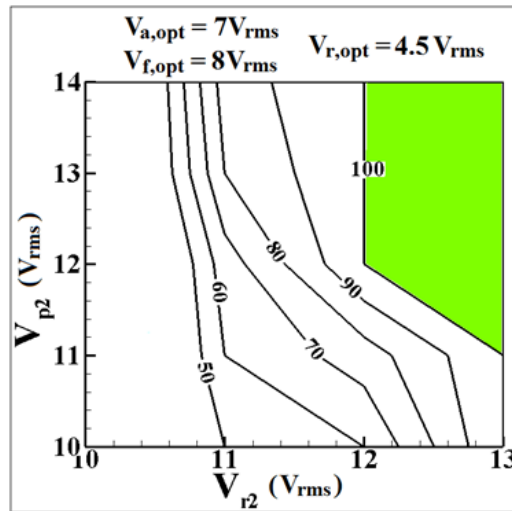
Figure 10. The trap function (performance cartography) of 2μm particles inside the second chamber in the new microchannel
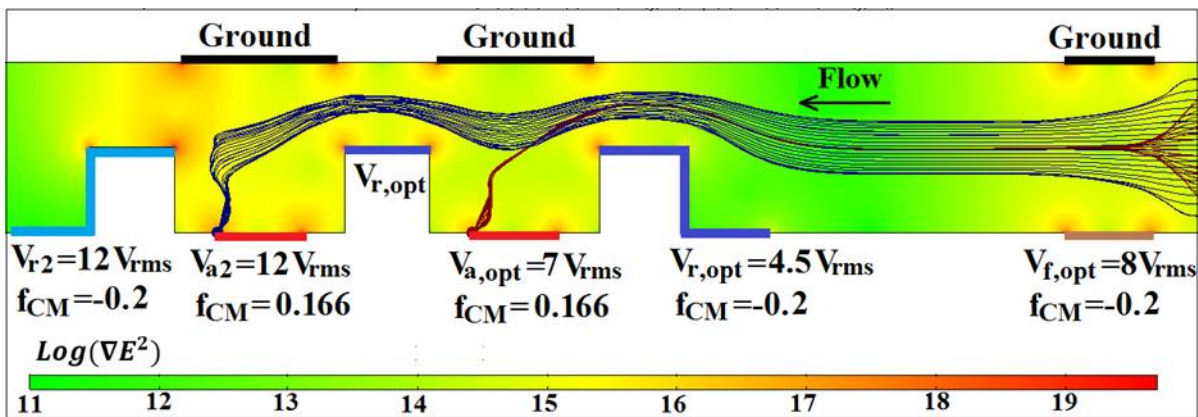
Figure 11. The motion path of 5μm (red) and 2μm (blue) polystyrene particles in the proposed microchannel

5. Conclusion

In this study, the process of simultaneous separation and trapping of particles as well as the dual trapping of particles have been conducted by using two frequencies of electric field. At first, the effects of frequency and voltage of electric field on trapping the 5μm polystyrene particles and ejecting the 2μm polystyrene particles in a single-chamber microchannel were investigated. In this situation, the performance of trapping the 5μm particles and ejecting the 2μm particles were calculated in terms of different values of voltage and frequency. Furthermore, the optimum voltages were obtained for 100% trapping of 5μm particles and the complete exit of 2μm particles. Then, a new microchannel consisting of two chambers was presented for dual trapping of 2μm and 5μm polystyrene particles at two different locations. In the new microchannel, the effect of voltage on trapping the 2μm particles in the second chamber was examined by selecting the optimum voltages that lead to 100% trapping of 5μm polystyrene particles in the first chamber. Thus, the performance of trapping the 2μm particles in the second chamber was attained, while the 5μm particles were trapped in the first chamber with 100% performance. The results reveal that a wide range of particles with different

sizes and electrical properties can be trapped at different locations by selecting the appropriate voltage and frequency.

Nomenclature

$\vec{x}_p$	Particle position (m)
$\vec{x}_0$	Initial particle position (m)
$\vec{u}_p$	Particle velocity (m/s)
$\vec{u}$	Fluid velocity (m/s)
t	time (s)
m_p	Mass of particle (Kg)
$\vec{F}_d$	Drag force (N)
$\vec{F}_{DEP}$	Dielectrophoretic force(N)
C_d	Friction factor (Kg/s)
R	Radius of particle (m)
f_{CM}	Clausius-mossoti factor
E_{rms}	Root mean square electric field (V/m)
p	Pressure (Pa)
V	Electric potential (V)
Greek Symbols	
μ	Dynamic viscosity of fluid (kg/m.s)
ε_0	Permittivity in vacuum (F/m)

ε_f	Relative permittivity of fluid
$\tilde{\varepsilon}_f$	Complex permittivity of fluid
$\tilde{\varepsilon}_p$	Complex permittivity of particle
σ	Electrical conductivity (S/m)
ω	Angular frequency (Hz)
ε_p	Complex permittivity of particle

References

[1] B.H. Weigle, R.L. Bardell, C.R. Cabrera, Lan-on-a-chip for drug development. Advanced Drug Delivery Reviews, 55(3), 349-377(2003)

[2] R. Langer, J.P. Vacanti, tissue engineering. Science, 260(5110), 920-926(1993)

[3] X.J. Feng, W. Du, Q.M. Luo, B.F. Liu, Microfluidic chip: next-generation platform for systems biology. Analytica Chimica Acta, 650(1),83-97(2009)

[4] K. Khoshmanesh, N. Kiss, S. Nahavandi, C.W. Evans, J.M. Cooper, D.E. Williams, D. Wlodkowic, Trapping and imaging of micron-sized embryos using dielectrophoresis. Electrophoresis, 32(22), 3129-3132(2011)

[5] G.J. Cheng, D. Pirzada, P. Dutta, Design and fabrication of a hybrid nanofluidic channel. J.Microlith. Microfab. Microsyst., 4(1), 013009(2005)

[6] S. Azimi, M. Nazari, Y. Daghighi, Developing a fast and tunable micro-mixer using induced vortices around a conductive flexible link. Physics of Fluids, 20(3), 032004(2017)

[7] S. Azimi, M. Nazari, Y. Daghighi, Fluid physics around conductive deformable flaps within an induced-charge electrokinetically driven microsystem. Microfluidics and Nanofluidics, 20(9), 124(2016).

[8] W. Waheed, A. Alazzam, B. Mathew, N. Christoforou, E. Abu-Nada, Lateral fluid flow fractionation using dielectrophoresis (LFFF-DEP) for size independent, label free isolation of circulating tumor cells. J. Chromatogr. B, 1087-1088, 133-137(2018).

[9] W. Norde, Colloids and interfaces in life science, second ed. Marcel Dekker, Monticello, NY, (2003).

[10] K.H. Kang, X.C. Xuan, Y.J. Kang, D.Q. Li, Effects of dc-dielectrophoretic force on particle trajectories in microchannels. Journal of Applied Physics, 99(6), 064702(2006)

[11] H.A. Pohl, Dielectrophoresis: the behavior of neutral matter in nonuniform electric fields, Cambridge University Press, Cambridge, New York, (1978).

[12] K. Zhao, L. Larasati, B.P. Duncker, D. Li, Continuous Cell Characterization and Separation by Microfluidic AC Dielectrophoresis. Anal Chem, 91(9), 6304-6314(2019).

[13] H.H. Cui, J. Voldman, X.F. He, K.M. Lim, Separation of particles by pulsed dielectrophoresis. Lab Chip, 9(16), 2306-2312(2009).

[14] T. Ye, H. Li, and K.Y. Lam, Two-dimensional numerical modeling for separation of deformable cells using dielectrophoresis. Electrophoresis, 36(3), 378-385(2015)

[15] C.M. Yousuff, N.H. Hamid, I. Hussain, E.T.W. Ho, Numerical Modelling and Simulation of Dielectrophoretic based WBC Sorting using Sidewall Electrode, 2016 6th International Conference on Intelligent and Advanced Systems (ICIAS), Kuala Lumpur, Malaysia, IEEE, pp. 1-5(2016)

[16] N. Piacentini, G. Mernier, R. Tornay, P. Renaud, Separation of platelets from other blood cells in continuous-flow by dielectrophoresis field-flow-fractionation. Biomicrofluidic, 5(3), 1-8(2011)

[17] J. Zhang, D. Yuan, Q. Zhao, S. Yan, S.Y. Tang, S.H. Tan, J. Guo, H. Xia, N.T. Nguyen, W. Li, Tunable particle separation in a hybrid dielectrophoresis (DEP)- inertial microfluidic device. Sensors and Actuators B: Chemical, 267, 14-25(2018).

[18] M. Hajari, A. Ebadi, M.J. Heydari, M. Fathipour, M. Soltani, Dielectrophoresis-based microfluidic platform to sort micro-particles in continuous flow. Microsyst. Technol., 26, 751-763(2020)

[19] J. Voldman, R. Braff, M. Toner, M. Gray, M. Schmidt, Holding forces of single-particle dielectrophoretic traps. Biophysical Journal, 80(1), 531-541(2001)

[20] D.V. Le, C. Rosales, B.C. Khoo, J. Peraire, Numerical design of electrical-mechanical traps. Lab Chip, 8(5), 755-763(2008)

[21] T. Zhou, J. Ge, L. Shi, J. Fan, Z. Liu, S. Woo, Dielectrophoretic choking phenomenon of a deformable particle in a converging-diverging microchannel. Electrophoresis, 39(4), 590-596(2017)

[22] V.H Perez-Gonzalez, R.C. Gallo-Villanueva, B. Cardenas- Benitez, S.O. Martinez-Chapa, B.H. Lapizco-Encinas, A simple approach to reducing particle trapping voltage in insulator-based dielectrophoretic systems. Anal Chem, 90(7), 4310-4315(2018).

[23] N. Demierre, T. Braschler, R. Muller, P. Renaud, Focusing and continuous separation of cells in a microfluidic device using lateral dielectrophoresis. Sensors and Actuators B: Chemical, 132(2), 388-396(2008)

[24] M. Urdaneta, E. Smela, Parasitic trap cancellation using multiple frequency dielectrophoresis, demonstrated by loading

cells into cages. Lab Chip, 8(4), 550-556(2008)

[25] B. Cetin, S.D. Oner, B. Baranoglu, Modeling of dielectrophoretic particle motion: Point particle versus finite-sized particle. Electrophoresis, 38(11), 1407-1418(2017)

[26] F.M. White, Fluid mechanic, McGraw-Hill Education, Boston, (2008).

[27] K.V.I.S. Kaler, J.P. Xie, T. Jones, R. Paul, Dual-frequency dielectrophoretic levitation of Canola protoplasts. Biophysical Journal, 63(1), 58-69(1992)

[28] A. Castellanos, A. Ramos, A. Gonzalez, N.G. Green, H. Morgan, Electrohydrodynamics and dielectrophoresis in microsystems: scaling laws. Journal of Physics D Applied Physics, 36(20), 2584-2597(2003)

[29] S.H. Beak, W.J. Chang, J.Y. Beak, D.S. Yoon, R. Bashir, S.W. Lee, Dielectrophoretic Technique for Measurement of Chemical and Biological Interactions. Analytical Chemistry, 81(18), 7737-7742(2009)

[30] G.H. Markx, R. Pethig, J. Rousselet, The dielectrophoretic levitation of latex beads, with reference to field-flow fractionation. Journal of Physics D: Applied Physics, 30(17), 2470-2477(1997)

.